Numerical Calculation of Nonlinear Aerodynamics of Wing-Body Configurations

Z. Rusak,* E. Wasserstrom,† and A. Seginer‡
Technion—Israel Institute of Technology, Haifa, Israel

A numerical method for the calculation of the nonlinear aerodynamic characteristics of wing-body configurations in steady low subsonic flow has been developed. The method is based on a combination of the linear source-panel method for the body and the nonlinear vortex-lattice method for the lifting surfaces and their separated wakes. Special emphasis is given to the understanding of the behavior and the computational accuracy of the numerical method. In order to demonstrate the capabilities of the present method, total and distributed loads are computed and compared with available experimental results. The computed examples cover simple configurations as well as more complicated geometries with greater relevance to modern missiles and aircraft. Details of the calculations clarify the significant nonlinear contribution of the body to the aerodynamic properties of the configuration. Good agreement was found between the computations and the experiments.

Nomenclature

a_{kl}, h_{kn}, b_k	= influence coefficients in Eqs. (7)
b	= wing span
B	= integration surface, Eq. (5)
C	= wing local chord
$\bar{C}$	= mean aerodynamic chord
C_l	= local airfoil lift coefficient
C_p	= pressure coefficient
$C_{L_{wc}}$	= lift coefficient of wing-canard in presence of body
C_M	= pitching moment coefficient relative to x_{ref}
C_{NOR}	= normal force coefficient
d	= maximum body diameter
m_l	= strength of a source panel l
n	= unit vector normal to the surface
N_k	= total number of vortex cells
N_s	= total number of source panels
r	= vector signifying distance
S_B	= body surface
S_W	= wing surface
u,v,w	= disturbance velocity components
U	= undisturbed freestream velocity vector
w	= wake surface
x,y,z	= Cartesian coordinates
x_{cp}	= center of pressure location
x_{ref}	= reference point for the pitching moment calculation
α	= angle of attack
Γ_n	= strength of the nth horseshoe vortex
ϕ	= disturbance velocity potential

Subscripts

s	= on the surface of the configuration
w	= on the vortex wake

Introduction

MODERN flight vehicles designed for transonic and supersonic flight often require complicated combinations of slender bodies and thin lifting surfaces with sharp leading and trailing edges. In a major part of their flight envelope the vehicles perform at subsonic speeds and high angles of attack. The desire for improved performance of missiles and aircraft leads to the widening of their operational envelope to even higher angles of attack. Therefore, the prediction of the aerodynamic characteristics of such configurations in this flight region is essential for their preliminary design stage.

High-angle-of-attack aerodynamics are characterized mainly by flow separations from various components of the vehicle. The wakes created contain strong concentrations of vorticity. The complexity of the three-dimensional flow pattern is caused by the interference between the lifting surfaces and the body, coupled with mutual interactions between these components and the vortex sheets. Consequently, the dependence of the aerodynamic properties on angle of attack is markedly nonlinear. The calculation of this nonlinear problem continues to present a challenge for aerodynamicists.

Over the years many analytical and numerical methods have been developed for the calculation of the aerodynamic properties of complicated wing-body configurations. In most of the available methods, only the linear potential flow is accounted for. The results obtained by these methods are therefore limited to unseparated flow and are applicable only at low angles of attack. Ashley and Rodden[1] and Thomas[2] have summarized and discussed these linear methods and their applications in subsonic and supersonic flows. The widely used panel methods, which solve potential unseparated flows past arbitrary three-dimensional configurations, are based on the integral formulation resulting from Green's theorem. Various combinations of sources, vortices, and doublet singularities have been used[3-10] to represent the bodies and the lifting surfaces. In these methods different options were used to simulate the lift carry-over induced by the wings on the body. These linear panel methods have matured over the last 25 years and have become a major design tool in the aeronautical industry. However, their predictions deteriorate at higher angles of attack, especially when flow separations occur.

In order to compute separated flows, panel methods for wings have been extended to include the rolled-up wakes. Such nonlinear methods for wings alone were developed by Kandil et al.,[11] Almonsino et al.,[12] Rebach,[13] and Johnson et al.[14] The vortex sheets emanating from the sharp leading edges and side and trailing edges were simulated either by free-vortex lines or free-doublet sheets. The agreement between the computed and experimental results for many wings

Received Feb. 18, 1982; revision received Nov. 8, 1982.

*Graduate Student, Department of Aeronautical Engineering.

†Associate Professor, Department of Aeronautical Engineering. Member AIAA.

‡Associate Professor, Department of Aeronautical Engineering (currently National Research Council Research Associate at NASA Ames Research Center). Member AIAA.

was quite good over a wide range of angles of attack, up to the onset of the vortex breakdown. These methods cannot, however, account for the body influence on the wing in wing-body configurations.

In actual airplane and missile configurations, the contribution of the body to the aerodynamic properties is significant. The estimation of the nonlinear wing-body interference by a superposition of solutions for isolated wings and isolated bodies is unsatisfactory. To demonstrate this point let us consider the missile configuration shown in Fig. 1.

The experimental pitching moment coefficient shown in this figure has a strong nonlinear variation with the normal force coefficient, and the static stability with respect to the chosen reference point changes sign from negative to positive as the angle of attack increases. The calculation of this configuration's aerodynamic properties using a linear potential attached flow method gives, as expected, good results only at low angles of attack.

A nonlinear vortex-lattice method (e.g., Ref. 12) when applied to the lifting surfaces alone (these have to be extended to the centerline of the configuration in order to account for the body contribution) describes the general character of the experimental results, but does not predict the correct values nor the exact variation in the static stability. The need for a method capable of treating the nonlinear wing-body interference of such a configuration is therefore obvious.

There exist only a few methods for the calculation of the nonlinear aerodynamics of wing-body configurations at high angles of attack. Mendenhall and Nielsen[15] applied the leading-edge suction analogy of Polhamus[16] to account for the nonlinear effects of the lifting surfaces. A crossflow theory combined with supplementary empirical data was used to approximately represent the nonlinear effects of the body. Only overall loads but no local load distributions could be predicted by this method. Nikolitsch[17] used a superposition of Wardlaw's two-dimensional multivortex model[18] for the nose tip flow separation and Gersten's approximate nonlinear method[19] for the exposed wing. The mutual interaction was considered separately for the body and wing. No free-wake calculations were made. This method was also limited to the prediction of the overall aerodynamic loads of simple central-wing-body combinations.

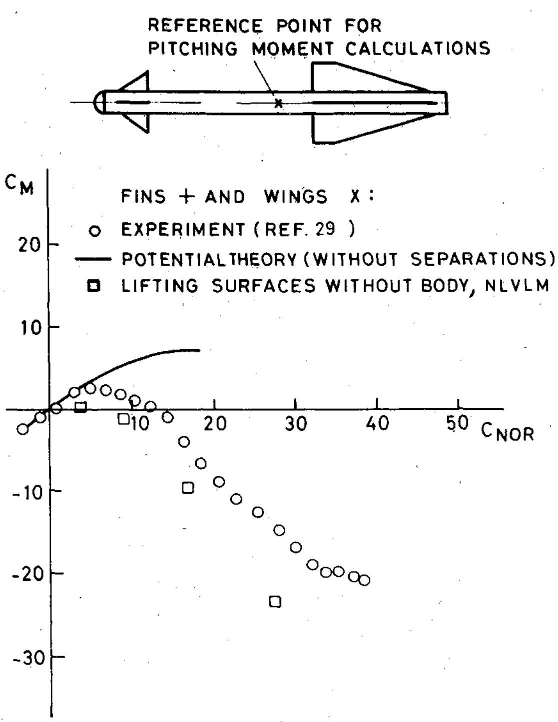

Fig. 1 Pitching moment coefficient vs normal force coefficient for a missile configuration.

In addition to these semiempirical methods, attempts were also made to extend the panel methods to treat the nonlinear flows around wing-body configurations. These, however, met with difficulties. Uchiyama et al.[20] suggested combining a nonlinear vortex lattice method for the lifting surfaces with concentrated sources to simulate the body. Mutual interaction was obtained from an iterative solution for the singularities strengths and the free-vortex pattern. However, the lift of the nose was still computed empirically and there was no mention of the way the lift carry-over of the body was accounted for. The method was applied to a very limited class of missile configurations and the results were not compared with either experiments or the other solutions. Atta and Nayfeh[21] extended the methods of Maskew[7] and Kandil et al.[11] to treat wing-body combinations. Their method used a potential flow model consisting of constant strength quadrilateral vortices distributed over the body and wing surfaces, thus accounting for interaction effects and flow separation from the lifting surfaces. However, only central-wing-body combinations, with small ratios of the body diameter to wing span, were considered. Computed results showed good agreement with experimental data up to the onset of the vortex breakdown. Johnson et al.[22] extended their own linear, high-order panel method[8] to a nonlinear potential flow scheme. The configuration surface was represented by source and doublet singularity panels, and the rolled-up vortex sheets and wake were modeled by doublet sheets. The strengths of the singularities, as well as the shape and position of the free-vortex sheet spirals, were computed iteratively, starting with an assumed initial sheet geometry based on the Mangler-Smith conical solution.[23] Computed results for the slender wings alone showed good agreement with experimental data. There is, however, no evidence in the literature of the application of this method to wing-body combinations.

The purpose of the present work is to develop a consistent numerical method for the treatment of complicated multiple-wing-body combinations at high angles of attack. The paper discusses the assumptions and considerations for choosing the model and the mathematical problem is formulated. The numerical implementation is described and the accuracy due to discretization errors is discussed. Finally, numerical results for two wing-body configurations are described and compared with experimental data.

Basic Assumptions

The main purpose of the present work was to develop a numerical method that could be used by the aeronautical industry as a tool for the preliminary design stage. Therefore, the method has to be sufficiently direct, simple to use, and efficient in order to be of practical engineering value. On the other hand, it was intended to have a reasonably sound mathematical basis and to avoid any usage of supplementary empirical information.

Since the nonlinear vortex-lattice method[12] proved to fit this description for isolated wings, it was a prime candidate for the present work. However, although it handled the vortex shedding from the wings quite well, it was doubtful if it could handle vortex shedding from the body as well. The mechanism of vortex shedding from an isolated body at high angles of attack is, in itself, not well understood, even from a fundamental point of view. Even the experimental evidence of the dependence of the characteristics of vortex shedding (such as the location of the separation lines on the body and the intensities of the free vortices and their trajectories) on parameters such as Mach number and Reynolds number is not decisive.[15,24] Furthermore, a general predictive method for the three-dimensional behavior of the vortices shed from the body is as yet unavailable.[25]

Experimental data[24,26,27] indicate that the direct contribution of the body vortices to the longitudinal aerodynamic coefficients of a wing-body configuration is generally small (although the vortices shed from the nose region may delay the breakdown of the wing vortices and thus postpone stall) and is usually limited to the nose region. Also, it was recently observed by Deane[24] and Jorgensen[26] that vortices shed by the nose can break down in the presence of a wing.

With the above-mentioned difficulties in mind (together with the experimental evidence concerning the relative unimportance of the direct contribution of the vortex shedding from the body to the longitudinal aerodynamic coefficients of the configuration), it was decided to simulate the body by a conventional source-panel method. The wings and all other lifting surfaces were simulated by the nonlinear vortex-lattice method that also accounted for the vortex shedding from all edges of the wing and for the wake roll-up. It was assumed that the nonlinear interference of wing-body combinations can be obtained by the simultaneous solution of the two systems solving for all the velocities induced by each one on the other.

Based on the successful results of this approach, it is assumed that the inclusion of a vortex field shed by the body in the computation (if a computational scheme for this case did exist) would not necessarily have improved the results, because of the experimentally observed[24] early breakdown of the body vortices in the presence of a lifting surface close to the nose.

Mathematical Formulation

A wing-body configuration is positioned at an angle of attack α in a uniform flowfield of an undisturbed velocity vector $\boldsymbol{U}_\infty$. The flow is assumed to be steady, incompressible, inviscid, and irrotational except for isolated vortices. The presence of the vehicle creates a disturbance velocity potential ϕ that is governed by the Laplace equation,

$$\nabla^2\phi = 0 \tag{1}$$

and by the boundary conditions on the vehicle surfaces and at infinity. On all solid surfaces the total velocity has to satisfy the tangency condition

$$\frac{\partial\phi}{\partial n_s} + \boldsymbol{U}_\infty \cdot \boldsymbol{n}_s = 0 \tag{2}$$

and the disturbance velocity has to vanish at infinity,

$$\nabla\phi \rightarrow 0 \quad \text{as} \quad |r| \rightarrow \infty \tag{3}$$

Several additional conditions have to be satisfied:

1) The vortex wakes w shed from the edges of the lifting surfaces are freestream surfaces, i.e., they are tangent to the total velocity at every point

$$\frac{\partial\phi}{\partial n_w} + \boldsymbol{U}_\infty \cdot \boldsymbol{n}_w = 0 \tag{4a}$$

and they cannot support a pressure jump

$$\Delta C_p \,|_w = 0 \tag{4b}$$

2) The aerodynamic load must satisfy a Kutta condition along all edges of the lifting surfaces that shed the separated vortices. This means that there cannot exist a pressure jump across the leading, trailing, or side edges of the wings.

Equation (1) and its boundary conditions constitute a mathematical formulation for the velocity potential ϕ. In spite of the Laplace equation being linear, the problem itself is nonlinear because of the unknown spatial trajectories of the free vortices. These have to be determined as part of the solution by the supplementary conditions [Eqs. (4)], thus rendering the problem nonlinear.

According to Green's theorem, any function ϕ that satisfies the integral equation,

$$\phi(x,y,z) = \frac{1}{4\pi}\iint_B \left[\phi\frac{\partial}{\partial n}\left(\frac{1}{r}\right) - \left(\frac{1}{r}\right)\frac{\partial\phi}{\partial n}\right]\mathrm{d}B \tag{5}$$

is a solution to Eq. (1), where ϕ is the disturbance potential at a point (x,y,z) in the flowfield and r the distance from this point to a point on the integration surface B that encloses all the singularities in the flowfield. The disturbance velocity potential of a specific wing-body configuration can be calculated from a distribution on the surface B of sources and/or dipoles of intensities $\partial\phi/\partial n$ and ϕ, respectively, that satisfies Eq. (5) and boundary conditions such as Eqs. (2-4).

In the present case, the surface B contains all the solid surfaces of the configuration (S_B for the body and S_W for the wings) and the free-wake surface w. Since it was assumed that the body in itself in nonlifting, its surface cannot support a jump in the potential of the disturbance velocity and is therefore described by a distribution of sources only.

The lifting surfaces, on the other hand, are described by a distribution of bound vortices that is equivalent to the appropriate dipole distribution and that describes the tangential velocity and potential jumps across the wings. Sources are not needed for the wings since their thickness is neglected. The trailing parts of the bound vortices simulate the vortex sheets shed by the wings. Since the free-vortex lines follow streamlines, according to the Helmholtz theorems, Eqs. (4) can be replaced by the streamline equations

$$\frac{\mathrm{d}y}{\mathrm{d}x} = \frac{v}{U_\infty + u}; \qquad \frac{\mathrm{d}z}{\mathrm{d}x} = \frac{w}{U_\infty + u} \tag{6}$$

Equations (1) and (3) are identically satisfied by the chosen distributions of singularities. The intensities of the singular elements and the trajectories of free trailing vortices are determined by a simultaneous solution of Eqs. (2) and (6). This represents a mathematically nonlinear problem of the close-coupled wing-body and wake solutions that is solved by an iterative procedure.

Method of Solution

The body surface is simulated by the linear source-panel method,[3] and the lifting surfaces with their shed vortex wakes are simulated by the nonlinear vortex-lattice method (NLVLM).[12] Any configuration of an arbitrary body and a number of symmetric wings can be simulated.

The body surface is divided into a number (N_s) of trapezoidal cells, each supporting a source distribution of uniform intensity m_l. A control point, at which the tangency boundary condition [Eq. (2)] is satisfied, is located at the center of the panel area. The lifting surfaces are divided into a number (N_k) of triangular and rectangular cells proposed by Almosnino et al.[12] (see Fig. 2 for a schematic division of a configuration into panels and cells). Each cell has a discrete horseshoe vortex of strength (Γ_n) bound to its quarter-chord line with the trailing vortices bound to the wing surface along the longitudinal cell demarcation lines until they reach one of the wing's edges. Free vortices are shed from all the wing edges (swept leading edge, side and trailing edges). The boundary condition control point on the vortex cells is located at the center of the cell three-quarters chord line.

An initial guess of the spatial trajectories of the free vortices is required to start the solution process. Semi-infinite straight lines, leaving the wing edges at some angle above the wing surface (e.g., ½α), are usually used. With the wake form predetermined, a simultaneous satisfaction of the tangency boundary condition [Eq. (2)] at all the control points results in

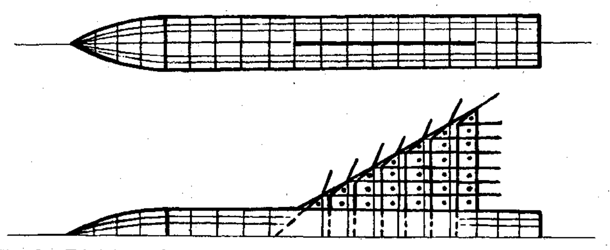

Fig. 2 Division of a wing-body configuration into panels and cells.

the following system of linear algebraic equations [Eqs. (7)] for the unknown intensities of the sources and vortices:

$$\sum_{l=1}^{N_s} a_{kl} m_l + \sum_{n=1}^{N_k} h_{kn} \Gamma_n + b_k = 0 \qquad (k=1,\ldots,N_s+N_k) \qquad (7)$$

where $b_k = (U_\infty \cdot n_s)_k$ is the component of the freestream velocity in the direction normal to panel or cell k at its control point, and a_{kl} and h_{kn} are the influence coefficients of source panel l and vortex n, respectively, on control point k. An influence coefficient is defined as the component, normal to panel k at its control point, of the velocity induced there $(\partial\phi/\partial n_s)_k$ by a singular potential element of unit strength at l or n. The detailed formulas for the influence coefficients are given in Ref. 28.

Equations (7) can be rewritten in a matrix form as

$$[BW]\Gamma + b = 0 \qquad (8)$$

where $[BW]$ is the influence coefficients matrix, Γ is the vector of singularity intensities $\Gamma = \{ {m_l \atop \Gamma_n} \}$ and b is the vector $b = \{b_k\}$.

Because of the structure of Eqs. (7), the matrix $[BW]$ can be partitioned into

$$[BW] = \begin{bmatrix} BOB & WOB \\ BOW & WOW \end{bmatrix} \qquad (9)$$

where BOB, WOB, BOW, and WOW represent, respectively, the influence coefficients of the body sources on the body panels, wing vortices on the body panels, body sources on the wing cells, and wing vortices on the wing cells.

The solution of Eq. (8) determines the strengths of the singular elements, which are then used to compute the velocities induced on the free vortices. Equations (6) are next integrated to determine the equilibrium trajectories of the force-free vortices in the wake. This is done using an Euler method that aligns vortex segments of predetermined length with the streamline direction. With the new wake shape determined Eq. (8) is then solved again for the new intensities of the sources and vortices, and the calculation cycle is reiterated. The solution is considered to be converged when the wake shape stops changing within a given tolerance.

Once the solution is converged, the load distribution on the wings and the pressure distribution on the body are computed using the Kutta-Joukowsky and Bernoulli equations, respectively, and the aerodynamic force and moment coefficients are calculated. Details of these calculations are presented in Ref. 28.

Wing-Body Intersection Problem

Hess[6] has already discussed the necessity to continue the vorticity distribution of the wing either on the body surface or through the body. The continuation of the vorticity distribution on, or through, the body may or may not represent the physical lift carry-over from the wings to the body. However, it eliminates the problem of a discontinuity in the vorticity distribution at the wing-body intersection line.

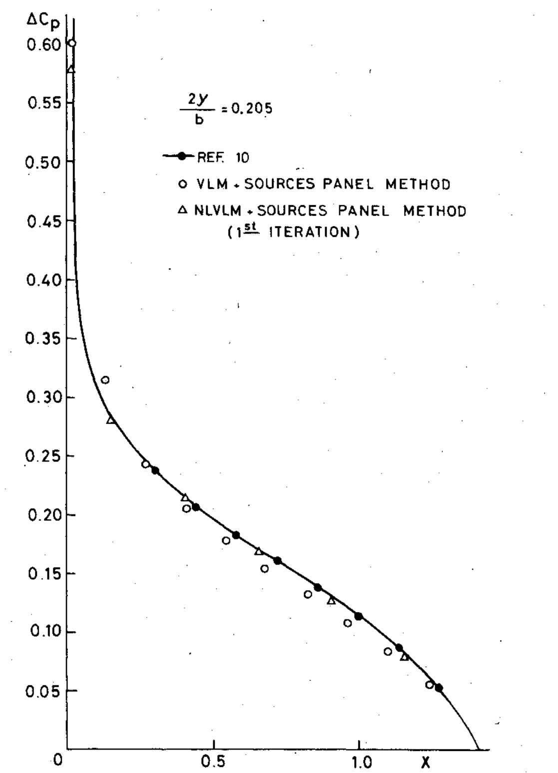

Fig. 3a Comparison between linear calculations: the pressure difference coefficient along a local chord of the wing near the wing-body intersection.

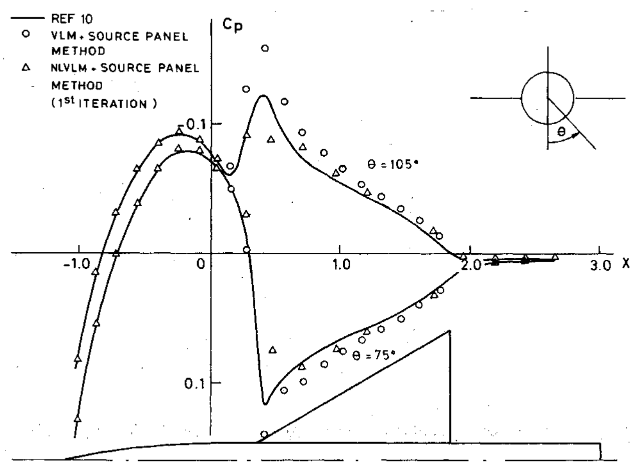

Fig. 3b Comparison between linear calculations: the pressure distribution over two longitudinal body strips above and below the wing.

Such a discontinuity in the mathematical model would cause the shedding of a strong vortex along this line. This vortex, which does not exist physically, would also encounter a strong interaction with the body because of its close proximity and would therefore pose numerical problems, preventing or delaying the convergence of the solution.

In the present work the vortex cells adjacent to the body are extended through the body up to the plane of symmetry. A vortex along the wing-body intersecton line is thus completely avoided. The velocities induced by the extended vortices are taken into account in the simultaneous solutions of Eqs. (6) and (8), but the tangency condition is not enforced on the extended panels. A similar approach was also used in the linear potential flow methods.[5,6,8-10] Forces acting on the extended vortices are not calculated, as the lift acting on the body is obtained from the pressure distribution.

Numerical Aspects of the Method

Before the method was applied to nonlinear problems, it was tested and proved for linear cases. First, the source-panel method for the body alone was successfully checked against analytical results for an ellipsoid.[28] Then, the complete computer program in its linear version (the first iteration only) was used to compute the pressure distribution over the wing-body configuration of Fig. 2 at a 6 deg angle of attack in incompressible flow. The body was an ogive cylinder with a fineness ratio of 8⅓, having a central delta wing of aspect ratio 2.31. The ratio of wing span to body diameter was 7.41. The computed results were compared with those of the proven IAIFLO linear code[10] (courtesy of the Israel Aircraft Industry) that uses source panels on the body and doublet panels on the wings, and with those of a combination of a source-panel model for the body and the classical linear vortex-lattice model (with trapezoidal cells) for the wings. The pressure difference across the wing, computed by the three methods, is presented in Fig. 3a at a spanwise station $y/(b/2)=0.205$, close to the wing-body intersection line. The pressure distribution over two longitudinal body strips above and below the wing is presented in Fig. 3b. Generally speaking, the results of the present method compare well with those of the more accurate panel method of Ref. 10. Some discrepancies exist at the wing leading edge (Fig. 3a) and near the intersection of the wing apex with the body (Fig. 3b); however, the strong pressure gradients that occur in these regions probably require a finer and denser panel/cell distribution. With the linear performance of the method accepted as satisfactory, attention was focused on the nonlinear behavior, namely the convergence characteristics of the method.

The typical convergence rate is demonstrated in Fig. 4, where the normal force and pitching moment coefficients of a representative cruciform wing-body configuration are presented as a function of the number of iterations. Only four iterations are needed to obtain the converged values of the aerodynamic coefficients (note the large change from the first to the second iteration). The pressure coefficient C_p (not shown in this figure) converges somewhat more slowly than the total aerodynamic coefficients. However, even the most sensitive parameter, the shape of the wake, is converged after seven iterations. The converged solution agrees fairly well with the experimental data of Ref. 29, especially with the pitching moment coefficient. The relative error in the normal force coefficient is less than 5% and the center of pressure is predicted within less than 10% of one body diameter.

The effects of several parameters (such as vortex-cell or source-panel size, the location of the boundary-condition control point, and the length of the free-vortex segments in the wake) on the convergence characteristics were also investigated. While full details of this investigation are described in Ref. 28 and will be published in a forthcoming paper, it is important to note here that a refinement of the computational grid leads to an asymptotic convergence only when a constant ratio of the cell size to wake segment length is maintained.

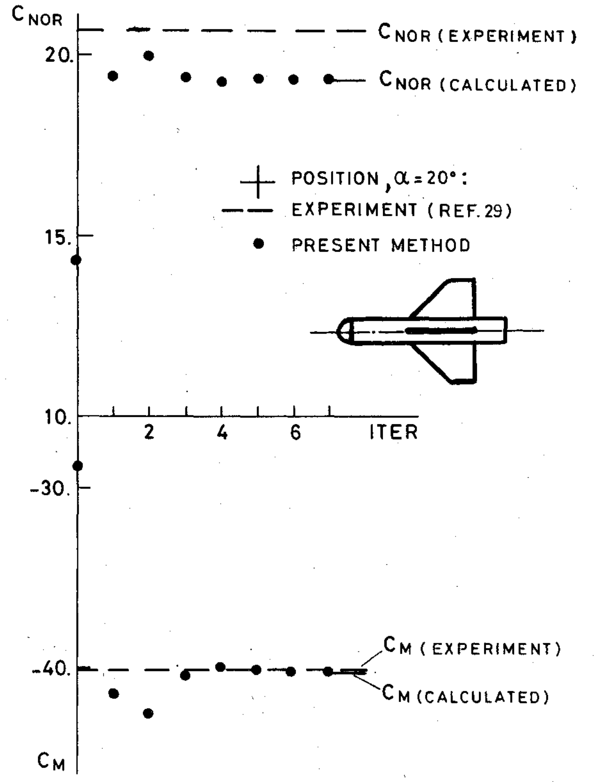

Fig. 4 Typical convergence of the iterative calculations of the overall loads for a wing-body combination.

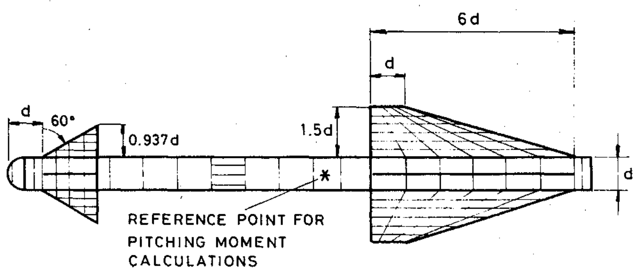

Fig. 5 Missile configuration geometry.

Results and Discussion

The present method was applied to several wing-body configurations, from simple to more complex ones. All the results are presented in Ref. 28. Only two configurations are discussed here. One is a typical missile configuration, while the other is typical of a modern fighter aircraft.

The first case is a missile configuration similar to the one described in Fig. 5. It has cruciform canard control surfaces in a (+) position and a cruciform wing rotated into an x position. This configuration was already mentioned in the Introduction, where it was shown (Fig. 1) that its aerodynamics cannot be predicted by existing nonlinear numerical methods. The calculated normal force coefficient and center-of-pressure location (relative to the reference point shown in Fig. 5) are compared in Fig. 6 with the experimental data of Ref. 29. Very good agreement is observed. Also shown for comparison are the results of the linear potential theory (solid line), which fit the data only for low angles of attack ($\alpha<6$ deg). The nonlinear contribution of the body to the normal force is certainly significant (Fig. 6). The calculated variation of the pitching moment coefficient (Fig. 7) is also in good agreement with the experimental data. The negative static stability at $\alpha<14$ deg relative to the indicated reference point, as well as the trim conditions are correctly predicted, while the linear potential theory can predict only the slope at small incidence. A nonlinear vortex-lattice (NLVLM) computation of all the lifting surfaces, including their parts that are buried in the body and are supposed to approximate the body aerodynamics, describes the data only qualitatively.

The breakdown of the overall aerodynamic coefficients is shown in Fig. 8. It is clearly seen that the body contributes to the lift as much as either pair of wings and about twice as much as the horizontal canard. It is also seen that the negative static stability of the configuration at low incidence (and its sign reversal at higher angles of attack) is due mainly to the body contribution to the positive pitching moment that levels off at higher angles of attack when the body center of pressure moves aft.

The second numerical example is presented for an aircraft-type configuration (Fig. 9). The configuration consists of an

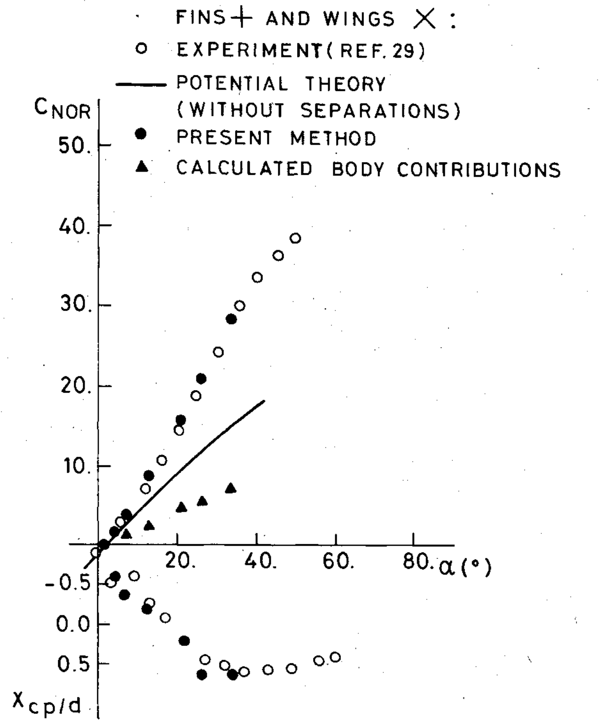

Fig. 6 Normal force coefficient and longitudinal center of pressure position vs angle of attack for the missile configuration.

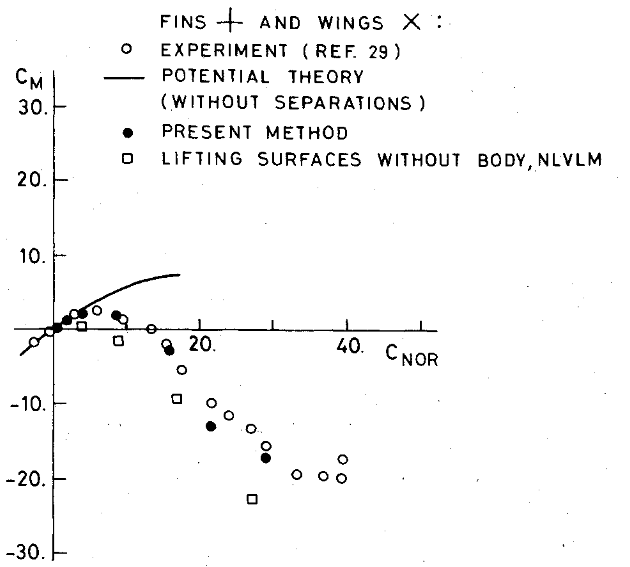

Fig. 7 Pitching moment coefficient vs normal force coefficient for the missile configuration.

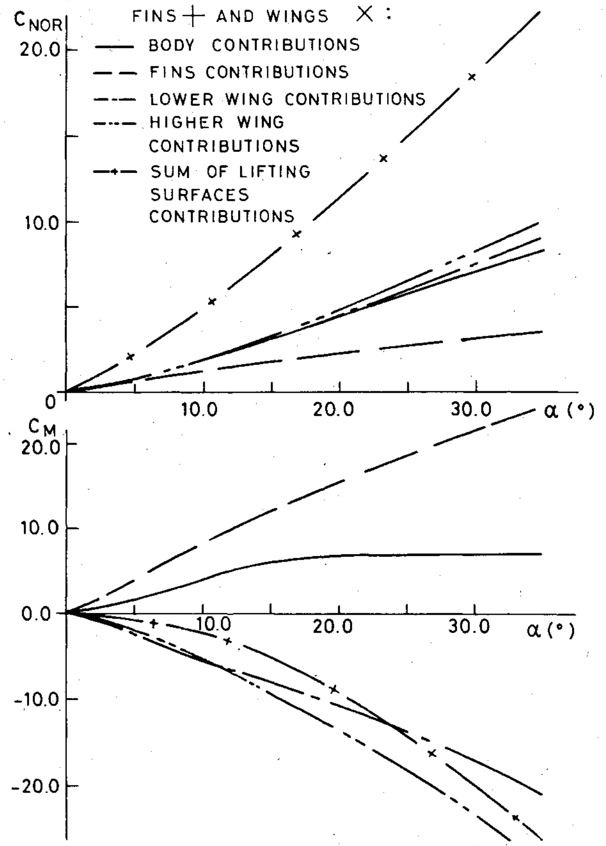

Fig. 8 Calculated lifting surfaces and body contributions to the normal force and pitching moment coefficients for the missile configuration.

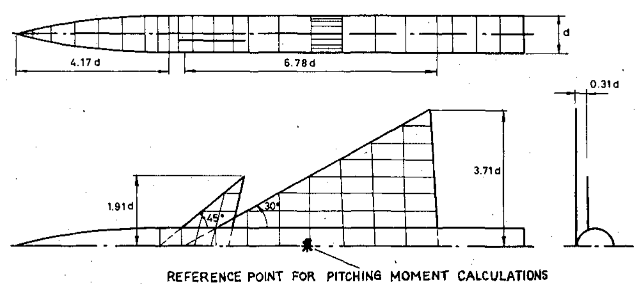

Fig. 9 Geometry of aircraft-type configuration.

ogive cylinder body, a sharp-edged, flat-plate, low delta wing of aspect ratio 2.17, and a sharp-edged, flat-plate, swept-delta canard positioned slightly below the body centerline. The normal force coefficient and the center-of-pressure location, calculated for the extended lifting surfaces only by the nonlinear vortex-lattice method (NLVLM[12]), are compared with the experimental data of Ref. 30 in Fig. 10. Although nonlinear, the calculated values of the normal force coefficient are too low, apparently due to the omission of the body. Also shown, to emphasize the nonlinearity of the results, is the straight line representing the lift curve slope at $\alpha = 0$ deg calculated by the linear theory. It is interesting that both the NLVLM and the linear theory correctly predict the location of the center of pressure.

The additional influence of the body on the configuration aerodynamics is shown in Fig. 11, where the normal force coefficient for the whole configuration calculated by the present method is in fair agreement with the experimental data. Presented separately are the accumulative contributions of the body, the wing, and the canard, each in the presence of the others. The relative influences of the components of the configuration on the wing and on the body are shown in Fig. 12. It is interesting to note that the presence of the body increases the wing lift (contrary to the linear theory prediction), and that the canard reduces it by an amount that is larger than the effect of the body. Even more interesting are the effects of wing and canard on the body (the lower curve in Fig. 12). While the wing induces a negative lift force on the body, its effect is not only cancelled, but reversed by a strong positive lift induced on the body by the canard. The results of the linear theory, also presented for comparison, show a qualitative agreement with the nonlinear results but have a different character.

Another interesting difference between the results of the linear and nonlinear approaches is found in the calculated spanwise distributions of the normalized section lift (a by-product of the calculation) that are presented in Fig. 13 for the wing-canard-body configuration at two angles of attack,

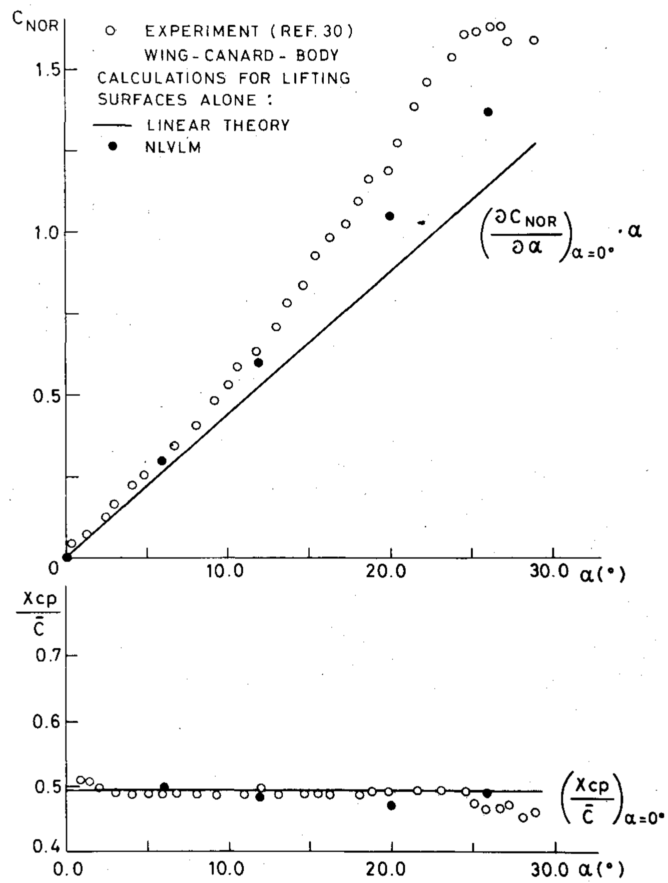

Fig. 10 Calculated normal force coefficient and longitudinal center of pressure location vs angle of attack (wing-canard without a body).

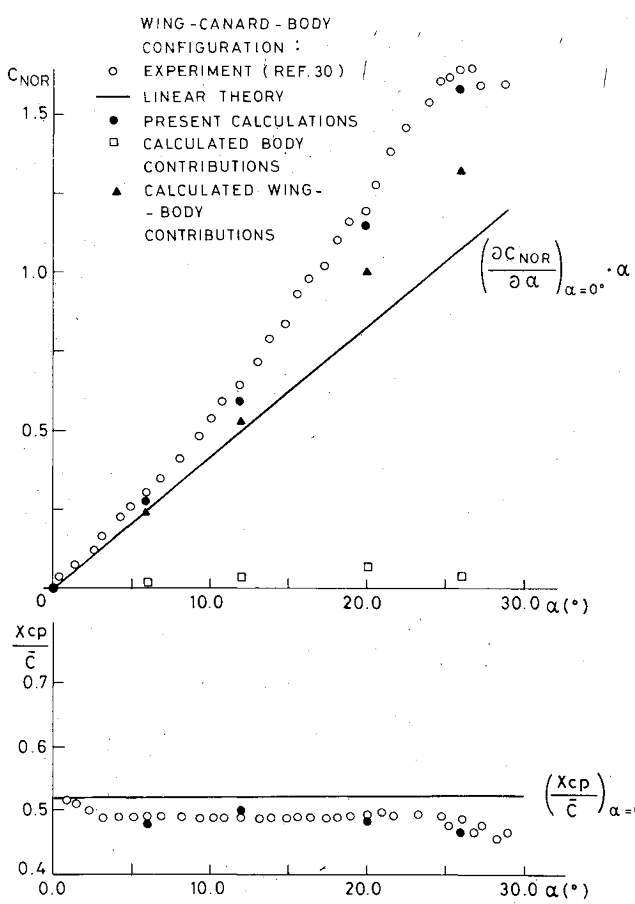

Fig. 11 Normal force coefficient and longitudinal center of pressure location vs angle of attack (wing-canard-body).

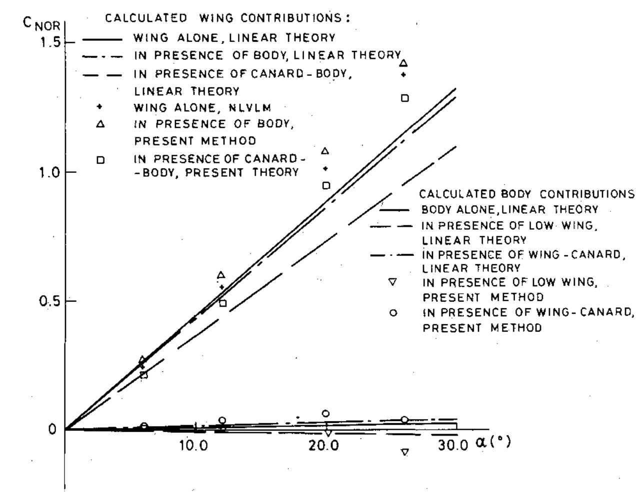

Fig. 12 Calculated wing and body contributions to the normal force coefficient in different combinations.

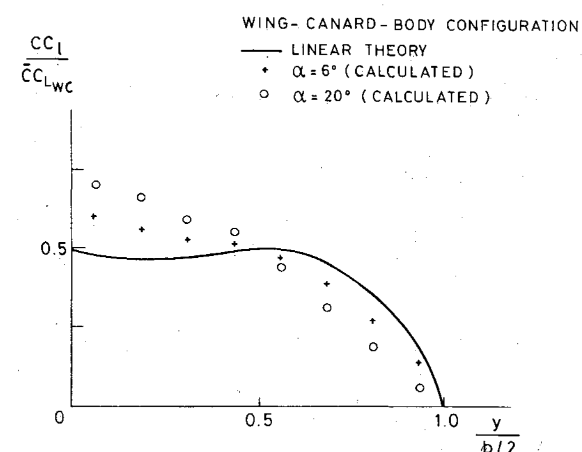

Fig. 13 Calculated spanwise load distribution for the wing in the aircraft-type configuration.

$\alpha = 6$ and 20 deg. While the linear theory predicts the maximum load somewhere around $y/(b/2) = 0.525$, the results of the present nonlinear computation show a reduction of the load on the outer half of the wing and an increase on the inner half. The maximum load occurs on the wing root. These effects increase with the total lift (or angle of attack). The same effects were observed[28] when the present method was applied to other wing-body configurations (without a canard) and also (in the NLVLM mode) to a delta wing alone. This is important information as far as the wing stall characteristics are concerned, and also for structural design purposes where the bending moment on the wing root is lower than the one predicted by the linear theory. Kraemer's experimental data (cited by Schlichting and Truckenbrodt in Ref. 31) for a wing alone also show this inward shift of the maximum load that is not predicted by the linear theory.

Conclusions

The method proposed in this paper computes the steady, incompressible potential flowfield around multiwing-body configurations at high angles of attack and is especially useful for the evaluation of their integral longitudinal aerodynamic properties, i.e., normal force and pitching moment coefficients, and the location of the center of pressure. The linear source-panel method is used to simulate the body and, consequently, bodies having arbitrary shapes can be treated. Lifting surfaces are simulated by a nonlinear vortex-lattice method that can handle leading-edge separation and a full rolled-up wake, which is best suited for application to very thin sharp-edged wings. The nonlinear contribution of the body induced by the wing is obtained by the simultaneous satisfaction of the flow tangency boundary condition on all the configuration surfaces. Comparison of the computational results with experimental data for both complicated missile and aircraft-type configurations showed good agreement, and proved that this method could be a useful engineering tool for the designer in the preliminary design stage when the aerodynamic characteristics of many diverse configurations have to be evaluated. No empirical information is required for such an evaluation. However, this does not include the induced drag which was also computed[28] but not presented here because of an additional empirical correction needed when the leading edge is not absolutely sharp.

The applicability of this method is naturally restricted to flight conditions where vortex breakdown has not yet occurred. Vortex breakdown apparently caused by viscous mechanisms and followed by loss of lift cannot be predicted by a potential theory. There is probably also a restriction on applicability, or a deterioration, of the computed results for configurations with very long slender noses at high angles of attack, where vortex shedding from the body cannot be neglected. However, such configurations, typical of fin-stabilized ballistic missiles, usually fly at low angles of attack anyway. For most highly maneuvering vehicles such as fighter aircraft or air-to-air missiles, the direct nonlinear nose effects on the longitudinal aerodynamic coefficients are apparently insignificant and the present method is applicable.

Acknowledgments

The work described here was done in partial fulfillment of the requirements for Master of Science degree of Z. Rusak. The authors would like to thank Prof. Rom, Dr. Gordon, and Dr. Almosnino for providing them with their NLVLM computer program and for many helpful discussions.

References

[1] Ashley, H. and Rodden, W. P., "Wing-Body Aerodynamics Interaction," *Annual Review of Fluid Mechanics*, Vol. 4, Annual Review Inc., Palo Alto, Calif., 1972, pp. 431-472.

[2] Thomas, J. L., "Subsonic Finite Elements for Wing-Body Combinations," *Vortex Lattice Utilization*, NASA SP-405, May 1976, pp. 11-26.

[3] Hess, J. L. and Smith, A.M.O., "Calculation of Potential Flow About Arbitrary Bodies," *Progress in Aeronautical Sciences*, Vol. 8, Pergamon Press, New York, 1967, pp. 1-138.

[4] Giesing, J. P., Kalman, T. P., and Rodden, W. P., "Subsonic Steady and Oscillatory Aerodynamics for Multiple Interfering Wings and Bodies," *Journal of Aircraft*, Vol. 9, Oct. 1972, pp. 693-702.

[5] Woodward, F. A., "An Improved Method for the Aerodynamic Analysis of Wing-Body-Tail Configurations in Subsonic and Supersonic Flow," NASA CR-2228, May 1973.

[6] Hess, J. L., "Calculation of Potential Flow About Arbitrary Three-Dimensional Lifting Bodies," McDonnell Douglas Corp., Rept. MDC J5679-01, Oct. 1972.

[7] Maskew, B., "Calculation of the Three-Dimensional Potential Flow Around Lifting Nonplanar Wings and Wing-Bodies Using a Surface Distribution of Quadrilateral Vortex-Rings," Loughborough University of Technology, Loughborough, England, Rept. TT-7009, Sept. 1970.

[8] Johnson, F. T. and Rubbert, P. E., "Advanced Panel-Type Influence Coefficient Method Applied to Subsonic Flows," AIAA Paper 75-50, Jan. 1975.

[9] Loeve, W., "On the Use of Panel Methods for Predicting Subsonic Flow About Airfoils and Aircraft Configurations," *Lecture Notes in Physics*, Vol. 59, Springer-Verlag, New York, 1976, pp. 75-83.

[10] Jacobs, A., Private communication, IAIFLO Computer Code, Israel Aircraft Industry, Ben-Gurion International Airport, Lod, Israel, 1982.

[11] Kandil, O. A., Mook, D. T., and Nayfeh, A. H., "Nonlinear Prediction of the Aerodynamic Loads on Lifting Surfaces," *Journal of Aircraft*, Vol. 13, Jan. 1976, pp. 22-28.

[12] Almosnino, D., Zorea, C., and Rom, J., "A Method for Calculating Longitudinal Characteristics of Wings and Multiple Lifting Surfaces in Subsonic Flow, and at High Angles of Attack," *Israel Journal of Technology*, Vol. 16, No. 3, 1978, pp. 132-141.

[13] Rehbach, C., "Numerical Investigation of Leading-Edge Vortex for Low Aspect-Ratio Thin Wings," *AIAA Journal*, Vol. 14, Feb. 1976, pp. 253-255.

[14] Weber, J. A., Brune, G. W., Johnson, F. T., Lu, P., and Rubbert, P. E., "Three-Dimensional Solution of Flows over Wings with Leading-Edge Vortex Separation," *AIAA Journal*, Vol. 14, April 1976, pp. 519-525.

[15] Mendenhall, M. R. and Nielsen, J. N., "Effect of Symmetrical Vortex Shedding on the Longitudinal Aerodynamic Characteristics of Wing-Body-Tail Combinations," NASA CR-2473, Jan. 1975.

[16] Polhamus, E. C., "Prediction of Vortex Lift Characteristics Based on a Leading-Edge Suction Analogy," AIAA Paper 69-1133, Oct. 1969.

[17] Nikolitsch, D., "Normal Force and Pitching Moment Coefficients of Bodies and Wing-Body Combinations at Very High Angle of Attack," AIAA Paper 78-63, Jan. 1978.

[18] Wardlaw, A. B. Jr., "Multivortex Model of Asymmetric Shedding on Slender Bodies at High Angle of Attack," AIAA Paper 75-123, Jan. 1975.

[19] Gersten, K., "A Non-Linear Lifting Surface Theory Specially for Low Aspect Ratio Wings," *AIAA Journal*, Vol. 1, April 1963, pp. 924-925.

[20] Uchiyama, N., Mikkilineni, R. P., and Wu, J. M., "The Analysis of Wing-Body Combinations at Moderate Angle of Attack," AIAA Paper 78-62, Jan. 1978.

[21] Atta, E. and Nayfeh, A. H., "Nonlinear Aerodynamics of Wing-Body Combinations," AIAA Paper 78-1206, July 1978.

[22] Johnson, F. T., Tinoco, E. N., Lu, P., and Epton, M. A., "Three-Dimensional Flow Over Wings with Leading-Edge Vortex Separation," *AIAA Journal*, Vol. 18, April 1980, pp. 367-380.

[23] Mangler, K. W. and Smith, J.H.B., "A Theory of the Flow Past Slender Delta Wing with Leading-Edge Separation," *Proceedings of the Royal Society of London*, Ser. A., Vol. 25, May 1959, pp. 200-217.

[24] Deane, J. R., "Wind and Water Tunnel Investigations of the Interaction of Body Vortices and the Wing-Panels of Missile Configuration," *High Angle of Attack Aerodynamics*, AGARD CP-247, Oct. 1978, pp. 18-1—18-8.

[25] Nielsen, J. N., "Missile Aerodynamics—Past, Present, Future," *Journal of Spacecraft and Rockets*, Vol. 17, May-June 1980, pp. 165-176.

[26] Jorgensen, L. H., "Prediction of Static Aerodynamic Characteristics for Slender Bodies Alone and with Lifting Surfaces to Very High Angles of Attack," NASA TR-R474, Sept. 1977.

[27] Akcay, M., Richards, B. E., Stahl, W., and Zarghami, A., "Aerodynamic Characteristics of a Missile Featuring Wing with Strakes at High Angle of Attack," *High Angle of Attack Aerodynamics*, AGARD CP-247, Oct. 1978, pp. 20-1—20-7.

[28] Rusak, Z., "Numerical Calculation of Wing-Body Configuration," MSc Thesis, Technion—Israel Institute of Technology, Haifa, Jan. 1982.

[29] Arielli, R., Unpublished experimental results, Technion—Israel Institute of Technology, Haifa, 1982.

[30] Liebermann, E. and Victor, M., Technion Research and Development Foundation, Haifa, Israel, Rept. 1-155, 4-133, and 9-109, 1972.

[31] Schlichting, H. and Truckenbrodt, E., *Aerodynamics of the Airplane*, McGraw-Hill Book Co., New York, 1979.